Quaternary Science Reviews 194 (2018) 116–127

Contents lists available at ScienceDirect

Quaternary Science Reviews

journal homepage: www.elsevier.com/locate/quascirev

Late Holocene activity of Sherman and Sheridan glaciers, Prince William Sound, Alaska

Dan H. Shugar [a, *], John J. Clague [b], Mauri J. McSaveney [c]

[a] Water, Sediment, Hazards and Earth-surface Dynamics (WaterSHED) Laboratory, School of Interdisciplinary Arts and Sciences, University of Washington Tacoma, Tacoma, WA, 98402, USA
[b] Department of Earth Sciences, Simon Fraser University, Burnaby, BC, V5A 1S6, Canada
[c] GNS Science, Lower Hutt, 6315, New Zealand

ARTICLE INFO

Article history:
Received 3 April 2018
Received in revised form
6 July 2018
Accepted 9 July 2018
Available online 17 July 2018

Keywords:
Sherman Glacier
Sheridan Glacier
Alaska
Climate change
Radiocarbon dating
Glacier-dammed lake
Holocene
Glaciation
Glacial geomorphology
Sedimentology

ABSTRACT

Two adjacent glaciers in the Chugach Mountains of south-central Alaska have markedly different histories on decadal to perhaps centennial timescales. Sheridan Glacier has advanced and retreated hundreds of metres during the latest Holocene. Its recent fluctuations have markedly altered local base level of Sherman River, which drains Sherman Glacier and flows into Sheridan Lake. Sheridan Glacier advanced to its greatest extent during the Little Ice Age, raising base level of Sherman River and inducing aggradation there of up to 17 m of sediment. Retreat of Sheridan Glacier formed a series of lakes that have coalesced. As lower lake outlets have become available, base level of Sherman River has dropped, resulting in the evacuation of substantial volumes of sediment from Sherman River valley. In about 2000, the terminus of Sheridan Glacier began to disintegrate; retreat accelerated dramatically in 2010. By 2016, the glacier had retreated an average of 600 m from its 2010 terminus, although some areas retreated up to 1.9 km and others did not retreat at all. Meanwhile, Sherman Glacier continued a slow advance initiated by a rock avalanche that blanketed much of its ablation area in the 1964 Alaska earthquake.
© 2018 Elsevier Ltd. All rights reserved.

1. Introduction

Glaciers are sensitive to changes in climate, but even adjacent glaciers can respond differently to climatic forcing. Depending on their size, alpine glaciers advance or retreat in response to a prolonged change in temperature or precipitation on timescales of a few years to several decades (Dyurgerov and Meier, 2000; Roe et al., 2017), but they can also be affected by other factors, for example whether they terminate on land or in the sea, or whether wind-blown snow is significant in their accumulation zones.

Nearly all alpine glaciers worldwide retreated in the twentieth century from their maximum Holocene extents achieved during the Little Ice Age (Grove, 2008). Exceptions include some tidewater glaciers in Alaska, whose regimen appears to be strongly affected by non-climatic factors (e.g. Mayo, 1989; Motyka and Echelmeyer, 2003), and some glaciers in the Karakoram that are gaining mass (Gardelle et al., 2012) following substantial mass loss since the Little Ice Age (Owen and Dortch, 2014). The amount of retreat and related glacier thinning is, in many cases, remarkable (e.g. Key et al., 2002; Moore et al., 2009; Bolch et al., 2010; Shugar et al., 2010; Bolch et al., 2012; Clarke et al., 2012) with ice volume losses in excess of 50% since the beginning of the twentieth century. Many small glaciers in marginally glacierized areas have disappeared entirely, for example in Glacier National Park in Montana. In some locations, the geomorphic response to glacier retreat has been swift, with at least one large river having been diverted (Shugar et al., 2017).

Barclay et al. (2013) describe fluctuations of four valley glaciers in coastal south-central Alaska over the past two millennia based on tree-ring and radiocarbon ages on glacially overridden stumps and logs. One of their records, for Sheridan Glacier, spans nearly 2000 years and, as those authors point out, is currently the most complete and best-constrained record of late Holocene glacier activity in Alaska. They identify four distinct phases of glacier advance

* Corresponding author.
E-mail addresses: dshugar@uw.edu (D.H. Shugar), jclague@sfu.ca (J.J. Clague), M.McSaveney@gns.cri.nz (M.J. McSaveney).

https://doi.org/10.1016/j.quascirev.2018.07.016
0277-3791/© 2018 Elsevier Ltd. All rights reserved.

at Sheridan Glacier: ca. 530 to 640, 1240 to 1280, 1510 to 1700, and 1810 to 1860 CE, which are broadly consistent with the main late Holocene intervals of glacier advance in Alaska described by other authors (Wiles et al., 2008; Solomina et al., 2015, 2016). Farther south in the British Columbia Coast Mountains, Hoffman and Smith (2013) describe three periods of advance at Bromley Glacier over the past 2000 years, at about cal. 30–330, 430–660, and 1040–1280 CE, while St-Hilaire and Smith (2017) describe advances at nearby Frank Mackie Glacier around cal. 250–660, 1450–1860, and 1700–1850 CE.

Here we add to this body of work with geomorphic mapping, stratigraphic analysis, and additional radiocarbon ages from the forefields of Sheridan and Sherman glaciers. We also provide a historical analysis of changes in the termini of the two glaciers using airphotos and satellite imagery dating from 1950 to 2016. We argue that Sheridan Glacier blocked Sherman valley several times during the past 1500 years, impounding a lake on each occasion. We show that a remarkably large volume of sediment was deposited in lower Sherman valley during the late Holocene and that much of this sediment has been removed since the Little Ice Age.

2. Regional setting

Sherman and Sheridan glaciers are adjacent, non-surging alpine glaciers in the Chugach Mountains near Cordova, Alaska (Fig. 1). Sherman Glacier is 13 km long, averages 2 km wide, and has a mean downvalley slope of ~2°. Its source area is about 650–1400 m above sea level (asl), and its terminus is at 150 m asl 11 km northwest of Copper River. Sheridan Glacier is 24 km long, has an average width of 2 km, and a mean downvalley slope of ~3°. Its source area is 750–1600 m asl; the glacier terminates in a proglacial lake at 90 m asl 14 km northwest of Copper River. Satellite imagery of the snowline position indicates the accumulation area ratios of Sherman and Sheridan glaciers were about 0.7, until recently. In the past decade, however, they have lowered to about 0.6.

Barclay et al. (2013) conclude that Sheridan Glacier dammed Sherman valley during an advance in the 1650s and 1660s, forming a shallow lake. Zander et al. (2013) inferred the activity of Sheridan Glacier based on cores collected from nearby Cabin Lake. They argue that the glacier briefly advanced from 11.2 to 11.0 cal Ka, and from cal. 1110 to 1180, 1260 to 1540, and 1610 to 1780 CE. There is, at best, imperfect overlap between these records and those of Barclay et al. (2013). The differences between these chronologies may result from the different approaches taken – glacially overridden and outwash-buried trees in the case of Barclay et al. (2013) and lake cores in the case of Zander et al. (2013). Further, Zander et al. (2013) point out that some advances of Sheridan Glacier may not have left a lacustrine sedimentary signature in Cabin Lake because the glacier's meltwater did not always enter the lake.

Sheridan Glacier was named during Abercrombie's (1900) expedition to the Copper River delta in 1884 and was first sketched by Seton-Karr and Bremner (1887, see Fig. 1). Early maps (Grant and Higgins, 1909; Hobbs, 1911) show Sheridan and Sherman glaciers as two tributaries feeding a single terminus, although Tarr and Martin (1914) later stated that Sherman Glacier was independent of its larger neighbour and that previous maps that showed the two as confluent were in error (see also Barclay et al., 2013). Wentworth and Ray (1936) confirmed that the two glaciers were separated by about 460 m in 1931, and they established a photo station near the terminus of Sheridan Glacier. We were unable to locate their photographs; the oldest photographs we found date to the 1950s.

Tarr and Martin (1914, p. 390) mention a mature coniferous forest just outside the terminus of Sheridan Glacier and suggest the glacier advanced prior to 1886 and had not retreated significantly by 1910. They make no mention of a proglacial lake at the Sheridan Glacier terminus or a glacier-dammed lake in nearby Sherman River valley. They do comment, however, that at the time of their survey Sheridan Glacier completely blocked the mouth of the valley draining Sherman Glacier, although it did not override a prominent rock knob on the east side of the Sheridan valley. They also suggest that Sherman Glacier had not advanced significantly in the nineteenth century, unlike Sheridan Glacier.

Based on field observations in 1926, Lutz (1930) describes recently abandoned moraine ridges about 150 m and 300 m from the Sheridan Glacier terminus. He observed 1.2-cm-tall mountain

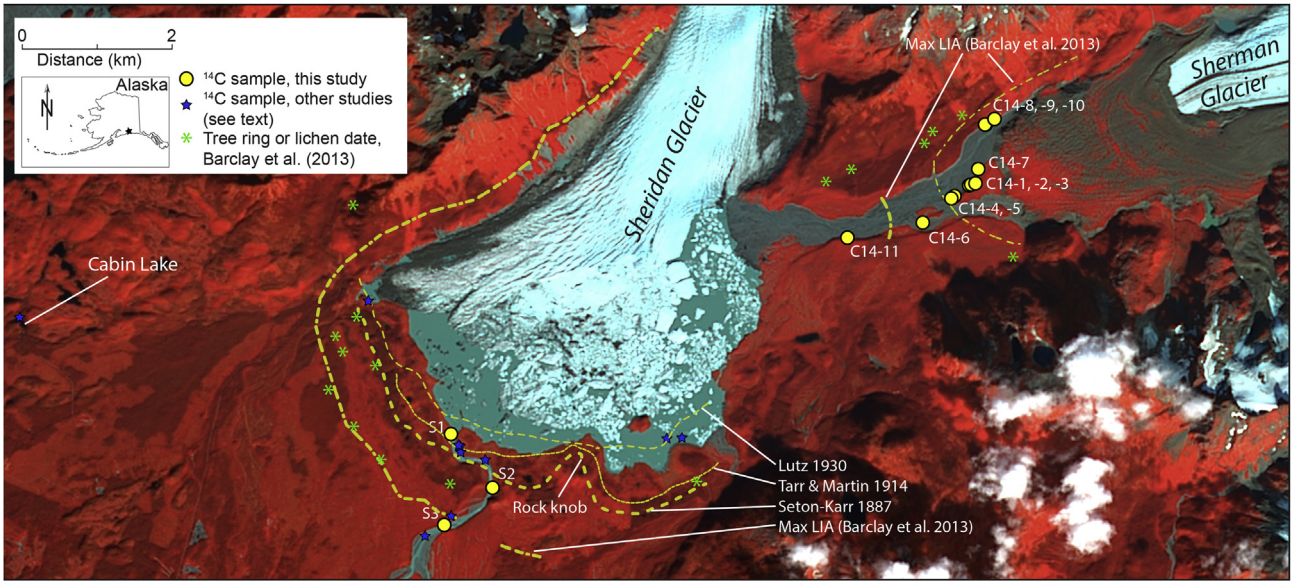

Fig. 1. Map showing the study area, radiocarbon and tree-ring locations, and Sheridan and Sherman glacier terminus positions from previous studies. Background is a Landsat 8 image (NIR-G-B) from September 7, 2015. Blue stars include radiocarbon-dated samples from Tuthill et al. (1968), Barclay et al. (2013), and Zander et al. (2013). Yellow circles represent locations of radiocarbon-dated samples of the current study. Yellow lines are approximate locations of glacier termini described by Seton-Karr and Bremner (1887), Tarr and Martin (1914), Lutz (1930), and Barclay et al. (2013). (For interpretation of the references to colour in this figure legend, the reader is referred to the Web version of this article.)

hemlock (*Tsuga mertensiana*) seedlings growing 100 m beyond the glacier terminus at the base of the most proximal moraine ridge. Based on this observation and assuming an ecesis time of 15 years (Wiles et al., 1999), Sheridan Glacier likely terminated at the inner moraine ridge described by Lutz (1930) around 1911 and retreated rapidly thereafter. Lutz (1930) also observed 20-cm-tall mountain hemlock and Sitka spruce (*Picea sitchensis*) on the outer side of this moraine and a 70- to 90-year old stand of Sitka spruce 335 m beyond the glacier terminus.

During the great Alaska earthquake on March 27, 1964, a large (~14×10^6 m^3) rock avalanche fell onto Sherman Glacier and blanketed ~8–8.4 km^2 of its ablation zone to depths averaging about 1.7 m with blocky greywacke and argillite debris (Marangunic and Bull, 1968; McSaveney, 1978; Shugar and Clague, 2011). Sheridan Glacier was unaffected by the landslide (Tuthill et al., 1968).

3. Methods

We mapped glacial landforms on satellite images and vertical aerial photographs. The mapping was field checked in 2008, and detailed stratigraphic and sedimentological observations were made in Sherman River valley between the termini of Sheridan and Sherman glaciers, and along Sheridan River southwest of Sheridan Glacier. Twenty-four samples of outer rings of rooted (in situ) tree stumps and stems, roots, and detrital logs were collected (Fig. 1) and AMS radiocarbon-dated. Calibrated ages are presented as 2σ ranges in calendric years CE, with a lab error multiplier of 2 using Calib 7.1 and the IntCal13 calibration curve. The entire calibrated age range is provided in the text where calibrations provided non-overlapping age ranges. For consistency, we have recalibrated previously published radiocarbon ages (e.g. Barclay et al., 2013) using the same method. Calibrated radiocarbon ages are rounded to the nearest decade and described as 'cal. CE', whereas tree-ring or historic (e.g. airphoto) dates are described as simply 'CE'.

We georeferenced vertical aerial photographs dating from 1950 to 1996 in ArcGIS using Digital Orthorectified Quadrangles flown in 1997 (Appendix 1). Each image was georeferenced with a minimum of 11 tie points using a third-order polynomial. Wherever possible, we selected tie points on flat terrain. The aerial photographs were supplemented with satellite imagery dating from 2000, 2010, and 2016. Glacier termini were digitized on the georeferenced imagery in ArcGIS.

We also used the 5-m-resolution ArcticDEM digital elevation model (DEM) created from optical stereo satellite photogrammetry to reconstruct a former glacier-dammed lake in Sherman River valley. Holes in the DEM were filled with the Elevation Void Fill raster function in ArcGIS. For this exercise, we inferred the location of the Sheridan Glacier terminus based on research by previous authors and us. The inferred terminus was modelled as a 100-m-high ice wall, which is similar to the thickness of the present glacier terminus. The terminus polygon was then converted to a raster and added to the ArcticDEM using Mosaic to New Raster in ArcGIS. We then reconstructed lakes that would form upvalley of the glacier dam by producing a contour map of the resultant topography and extracting the highest contour line that fully enclosed the lake basin. We acknowledge that the DEM represents the modern land surface in Sherman valley, which is not the surface at the time the lake formed.

4. Stratigraphy and chronology

We infer at least five advances of Sheridan Glacier based on the data presented below. These include the First Millennium advance identified by Barclay et al. (2013), one early Second Millennium advance, and at least three Little Ice Age advances. As described below, other workers have identified at least two other postglacial advances of Sheridan Glacier. We found evidence for only two Little Ice Age advances of Sherman Glacier, consistent with findings of previous workers.

4.1. First Millennium Advance

The oldest in situ subfossil trees that we found are located along Sheridan River at the current outlet of its proglacial lake (Sheridan 1, cal. 220–380 CE, Table 1; Fig. 2) and 360 m downstream (Sheridan 2A, ~210 rings, outer rings cal. 430–620 CE; Sheridan 2B, cal. 540–720 CE). The Sheridan 1 sample is buried in outwash gravel and boulders (Fig. 2B).

Horizontal logs and roots occur within till in an exposure between Sheridan and Sherman glaciers about 1.4 km east of the current margin of Sheridan Glacier. Three samples (C14-11B, 11D, and 11E, Fig. 1) yielded similar radiocarbon ages, with a calibrated age range of cal. 400–640 CE. This age range overlaps that obtained on samples from sites Sheridan 2A and 2B, described above. Gravel beds dipping westward toward Sheridan Glacier overlie the dated till and may record deposition in a lake impounded by that glacier in the lower part of Sherman valley.

4.2. Second Millennium and Little Ice Age

4.2.1. Sheridan Glacier

The maximum Little Ice Age extent of Sheridan Glacier lies beyond all except one of our dated sample sites in Sheridan valley (i.e., site Sheridan 3, Figs. 1 and 3). Sheridan 3 is a 15-m-high bluff located on the northwest side of Sheridan River about 1.5 km southwest of the outlet of the current lake. Most of the section is Sheridan Glacier outwash gravel, but three poorly developed soils with rooted tree stumps and stems are present about 8.5, 9.5, and 13 m above river level (Fig. 3).

The lowest exposed sediment is poorly sorted, pebble-cobble gravel with rounded to subrounded stones up to 2 m in diameter. This gravel is overlain 8.5 m above the level of the river by, successively, a thin peat layer, 30 cm of olive-grey silt, and 20 cm of sand, sandy silt, and pebbly sand, in which stumps and tree stems up to 2 m tall and 20 cm in diameter are rooted. Outer rings of two of the stumps date to cal. 1290–1410 CE and cal. 1460–1640 CE (Sheridan 3A and 3B, respectively). Sheridan 3A must have died for reasons unrelated to a glacier advance, because the range of possible kill dates of Sheridan 3B postdates it. However, it still provides a limiting (minimum) age for the establishment of the soil. A thin rooting horizon lies about 1 m above this soil. An in-situ root from this horizon yielded an age of cal. 1480–1660 CE (Sheridan 3C). Another gravel unit, about 3 m thick, overlies this thin soil and, in turn, is capped by a soil with large in-situ stumps and stems of trees up to 1 m in diameter and 3 m tall. Some of the vertical stems extend above the level of the terrace surface, which is about 1.5 m above the rooting level. Outer rings of one of the stems yielded calibrated radiocarbon age ranges of cal. 1680–1740 CE and cal. 1800–1940 CE (Sheridan 3D). The age must be closer to the lower end of this range than the upper end because logged trees on the terrace surface above the section were about 200 years old when harvested (clear-cut logging occurred between the mid-1980s and 1994). The trees are buried by about 1.5 m of horizontally stratified, sandy gravel and clast-supported diamicton with stones up to 1 m in diameter.

Assuming that the gravel units are outwash deposited at times when Sheridan Glacier was advancing, the Sheridan 3 section provides evidence for four Holocene advances of the glacier – the first before cal. 1290 CE; a second after cal. 1460 CE but prior to 1480

Table 1
Radiocarbon ages from the forefields of Sheridan and Sherman Glaciers.

Sample name	Radiocarbon age (BP)	Calibrated age range (CE)[a]	Lab number[b]	Easting	Northing	Elev (m asl)	Notes
		Sheridan Lake					
Sheridan 1	1750 ± 15	220–380 (1.0)	Keck-54545	590310	6709842	40	Outer rings of semi-submerged, rooted stump
n/a	2830 ± 100	1500 BC – 510 BC (0.999)	I-1985	593185	6709740	45	Sample of log buried in lake sediment from Tuthill et al. (1968)
n/a	1610 ± 100	40 BC – 780 (0.989)	I-1986	593390	6709740	43	Sample of glacier-transported log, from Tuthill et al. (1968)
n/a	1130 ± 100	560–1270 (1.0)	I-1987	589200	6711580	44	Sample of buried rooted stump, from Tuthill et al. (1968)
		Downstream of Sheridan Lake, along Sheridan River					
Sheridan 2A	1515 ± 15	430–500 (0.255) 530–620 (0.724)	Keck-54546	590863	6709130	39	Outer rings of rooted stump previously cut with chainsaw
Sheridan 2B	1400 ± 30	540–720 (0.958)	Beta-296737	590863	6709130	39	Outer rings of rooted stump previously cut with chainsaw
Sheridan 3A	605 ± 20	1290–1410 (1.0)	Keck-54547	590216	6708632	43	Outer rings of stratigraphically lowest rooted tree stem
Sheridan 3B	350 ± 20	1460–1640 (1.0)	Keck-54548	590216	6708632	43	Outer rings of stratigraphically lowest rooted tree stem
Sheridan 3C	295 ± 20	1480–1660 (0.997)	Keck-54549	590216	6708632	43	Root in upper rooting horizon immediately above Sheridan 3A, 3B
Sheridan 3D	95 ± 20	1680–1740 (0.278) 1800–1940 (0.691)	Keck-54550	590216	6708632	43	Root of large in situ tree near top of section
n/a	650 ± 120	880–1690 (0.963)	I-1689	590410	6709675	49	Stump buried in outwash; Tuthill et al. (1968)
n/a	455 ± 125	1150–1950 (0.992)	I-1690	590410	6709675	49	Stump buried in outwash; Tuthill et al. (1968)
n/a	480 ± 125	1150- 1950 (0.980)	I-1691	590425	6709645	47	Rooted stump on terrace on E side of river; Tuthill et al. (1968)
n/a	550 ± 95	1040–1680 (0.961)	I-1984	590435	6709555	38	Rooted tree tipped downstream; Tuthill et al. (1968)
n/a	230 ± 100[c]	1390–1950 (0.989)	I-1692	590863	6709130	39	Rooted stump buried in outwash; Tuthill et al. (1968)
n/a	370 ± 115	1270–1950 (1.0)	I-1693	590230	6708585	37	Rooted stump buried in outwash; Tuthill et al. (1968)
n/a	1670 ± 75	50–650 (1.0)	CURL-5294	590754	6709444	40	Single growth ring from same situ stump as CURL-5298 (site 'D'), cross dated as 311 CE.
n/a	1670 ± 40	210-560 (0.977)	CURL-5298	590754	6709444	40	Single growth ring from same situ stump as CURL-5294 (site 'D'), cross dated as 432 CE.
n/a	800 ± 60	1020–1400 (1.0)	Beta-98985	590300	6708718	33	Outer rings of in situ stump (site 'F').
n/a	230 ± 60	1470–1950 (1.0)	Beta-98986	590300	6708718	33	Outer rings of stump (site 'F').
		Sherman Glacier outwash plain					
C14-1	280 ± 15	1510–1600 (0.566) 1620–1670 (0.403)	Keck-54542	597227	6713164	96	Outer rings of rooted stump
C14-2	340 ± 20	1460–1640 (1.0)	Keck-54543	597254	6713170	95	Outer rings of rooted stump
C14-3	265 ± 20	1490–1680 (0.868) 1760–1800 (0.110)	Keck-54605	597308	6713190	96	Outer rings rooted stump
C14-4	220 ± 20	1632–1694 (0.355) 1726–1813 (0.473) 1920–1950 (0.130)	Keck-54606	597027	6713020	94	Outer rings of horizontal tree stem
C14-5	290 ± 20	1480–1670 (0.982)	Keck-54607	596985	6712987	94	Outer rings of stump that slid down face
C14-6	225 ± 20	1520–1570 (0.055) 1630–1690 (0.378) 1730–1810 (0.448) 1920–1950 (0.119)	Keck-54608	596604	6712666	89	Outer rings of horizontal log
C14-7	365 ± 20	1450–1640 (1.0)	Keck-54609	597346	6713378	101	Outer rings of rooted stump on floodplain. Stump is farthest northeast along Sherman River.
		Between Sherman and Sheridan glaciers					
C14-11B	1580 ± 20	400-570 (1.0)	Keck-54610	595602	6712461	75	Outer rings of log
C14-11D	1520 ± 20	430-620 (1.0)	Keck-54611	595602	6712461	75	Root of tree
C14-11E	1505 ± 15	430-640 (1.0)	Keck-54544	595602	6712461	75	Root of tree
		North side of Sherman River					
C14-8	273 ± 20	1490–1670 (0.922) 1780–1800 (0.067)	GNS-65424	597448	6713974	125	Outer rings of rooted stump
C14-9 outer[d]	104 ± 20	1680–1760 (0.327) 1800–1940 (0.673)	GNS-65430	597438	6713974	127	Ring 65 of rooted tree stem
C14-9 mid[d]	227 ± 20	1520–1570 (0.065) 1630–1690 (0.386) 1730–1810 (0.435) 1920–1950 (0.114)	GNS-65429	597438	6713974	127	Ring 26 of rooted tree stem
C14-9 inner[d]	206 ± 20	1640–1700 (0.293) 1720–1820 (0.514) 1920–1950 (0.154)	GNS-65428	597438	6713974	127	Ring 4 of upright stem

(*continued on next page*)

Table 1 (*continued*)

Sample name	Radiocarbon age (BP)	Calibrated age range (CE)[a]	Lab number[b]	Easting	Northing	Elev (m asl)	Notes
C14-10a[e]	225 ± 20	1520–1570 (0.055) 1630–1690 (0.378) 1730–1810 (0.448) 1920–1950 (0.119)	GNS-65425	597565	6714045	121	Outer rings of rooted stem
C14-10b[e]	183 ± 20	1650–1710 (0.220) 1720–1820 (0.516) 1830–1880 (0.093) 1910–1950 (0.171)	GNS-65426	597565	6714045	121	Outer rings of rooted stem
C14-10c[e]	209 ± 20	1640–1700 (0.306) 1730–1820 (0.508) 1920–1950 (0.150)	GNS-65427	597565	6714045	121	Outer rings of rooted stem
n/a	1180 ± 40	680–990 (1.0)	CURL-5297	597625	6714045	117	Single growth ring from in situ stump dated by Barclay et al. (2013).

[a] 2σ calibrated age ranges, rounded to nearest decade. Calibrated ages were determined using Calib v 7.1 with the IntCal13 calibration curve (Bronk Ramsey, 2009) and an error multiplier of 2. Only ranges with probability distributions >0.05 are shown, with probabilities given parenthetically. In cases where discontinuous calibrated age ranges are separated by less than a decade, they are listed as continuous.
[b] Labs: Beta – Beta Analytic Inc; GNS – GNS Science; KECK – University of California Irvine Keck Carbon Cycle AMS Laboratory; CURL – University of Colorado Boulder.
[c] No uncertainty provided by Tuthill et al. (1968). We have assumed an uncertainty of ±100 y, based on their other samples.
[d] C14-9-outer, C14-9-mid, and C14-9-inner are samples from a single tree.
[e] C14-10a, C14-10b, and C14-10c are samples from three closely spaced trees 3–4 m above the floodplain.

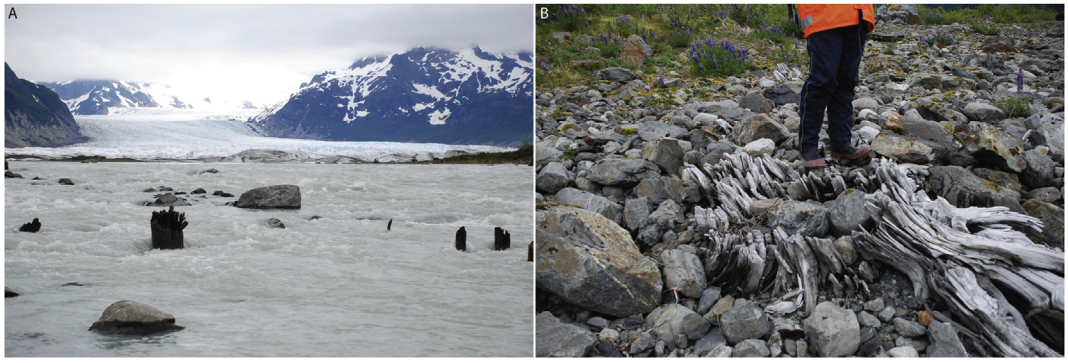

Fig. 2. A) Tree stems in growth position at the outlet of Sheridan Lake and B) an in-situ stump at site Sheridan 1 at the lake outlet (see Fig. 1 for locations).

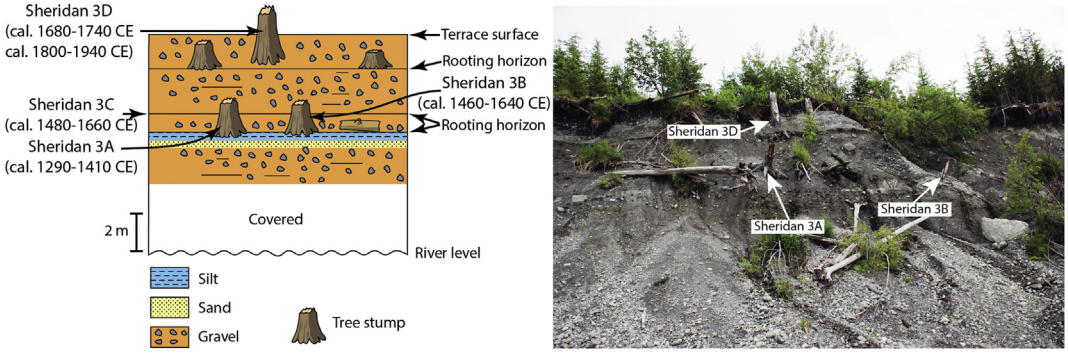

Fig. 3. Schematic illustration and photograph of the Sheridan 3 section on Sheridan River.

CE; a third after cal. 1480 CE but prior to 1680 CE; and a fourth after cal. 1680 CE but before the late 1700s CE. A tree dated by Barclay et al. (2013) at their site E (near our Sheridan 2), was killed by advancing Sheridan Glacier between 1279 and 1284 CE.

4.2.2. Sherman Glacier

We dated outer rings of stumps in growth position on the modern floodplain of Sherman River and horizontal stems and horizontal tree stems in a low terrace bordering the river (samples C14-1 through C14-7, Fig. 1). The calibrated radiocarbon ages range from cal. 1450 to 1950 CE. Samples C14-1 (cal. 1510–1670), C14-2 (cal. 1460–1640 CE), and C14-3 (cal. 1490–1800) are rooted 2 m above the current river level about 500 m from the terminus of Sherman Glacier (Fig. 1). If these trees all died at the same time due to burial by outwash at a level 2 m above present river level, the kill date must be between cal. 1510 and 1640 CE. Sample C14-7 (cal. 1450–1640 CE) is rooted within 1 m of current river level about 350 m from the glacier terminus. Samples C14-4 (cal. 1630–1950 CE) and C14-5 (cal. 1480–1670 CE) are tree stems another 450 m downvalley from the 2008 glacier terminus. These two samples lie

on the same surface as samples C14-1, C14-2, and C14-3, but are buried beneath nearly 2 m of horizontally stratified, pebble-cobble-boulder gravel with stones up to 0.6 m in diameter. The top of this gravel unit is a terrace incised into a nearly 20-m-thick Sherman Glacier valley fill. The tree stems, which are up to 10 m long, extend horizontally out of the bank. They lie on 7 cm of olive-grey clayey silt, which in turn overlies dark brown to rusty, pebble-cobble gravel with stones up to 0.3 m in diameter. The olive-grey silt, although thin, may be a lacustrine deposit, laid down in an ice-dammed lake impounded by an expanded Sheridan Glacier. A second higher terrace lies ~3 m above the first.

Many tree stems up to 3 m tall are rooted on the bedrock slope on the north side of Sherman River near the glacier terminus (Fig. 4). The stems occur over a vertical range of 2–8 m above current river level and have been exhumed from horizontally stratified pebble-cobble-boulder gravel that extends discontinuously to a terrace ~17 m above river level. Samples C14-8 (outer rings cal. 1490–1800 CE) and C14-9 (outer rings cal. 1680–1940 CE) are from the same level, 4 m above river level. C14-9 is a stem with about 65 rings rooted in a 7-cm-thick brown peat that lies on bedrock. This stem yielded three ages: the outer ring described above, a second of cal. 1520–1950 CE on middle rings, and cal. 1640–1950 CE on an inner ring near the pith. Samples C14-10A, B, and C are the outer rings of three closely spaced stems rooted 3–4 m above river level. The ages of these samples fall within the range cal. 1650–1950 CE. Barclay et al. (2013) provide tree-ring dates on five stumps from the same area, which record growth from 1512 until about 1820 CE.

Fig. 4. Photographs of rooted stems on north side of Sherman River near the terminus of Sherman Glacier. Dashed box in (A) shows approximate location of (B).

Considering an earliest kill date for C14-9 of cal. 1705 CE (based on a ring count of ~65 and the maximum inner ring radiocarbon age of cal. 1640 CE, we posit that Sherman Glacier could not have extended downstream more than about 350 m beyond its present limit prior to cal. 1640 CE until at least sometime after cal. 1705 CE, which is in agreement with the findings of Barclay et al. (2013) who suggest the glacier was retracted from at least 1512 CE to about 1820 CE. It is unlikely that the trees were killed directly by overriding ice, but rather were buried by outwash. It is conceivable that outwash buried multiple trees, killing them simultaneously. These could then have been overridden by advancing Sherman Glacier in the early 1800s CE (c.f. Barclay et al., 2013). The outwash in this case would have protected the trees until they were exhumed in the twentieth century. The trees shown in Fig. 4 indicate that they may have been trimmed at the same level by the advancing glacier. Sometime after cal. 1705 CE, at least 17 m of gravelly outwash were deposited on the valley floor downstream of the glacier terminus.

4.3. Historic activity

The terminus of Sheridan Glacier fluctuated significantly over the period spanned by aerial photographs and satellite imagery (1950–2016 CE; Fig. 5). Most of the terminus in 1950 was about 0.5–0.6 km downvalley of its position in 2000; at one location, it was more than 1 km downvalley. Between 1950 and 1959, the south and southwest margins of the glacier changed little, while the eastern margin retreated up to 0.5 km. Sheridan Glacier retreated up to 0.4 km between 1959 and 1974, and up to about 0.2 km between 1974 and 1996, except along its east margin along the Sherman outwash plain where it retreated about 0.7 km. Between 1996 and 2000, the terminus remained stationary over much of its perimeter, although it advanced locally up to about 0.2 km. A small, but prominent bedrock island in the east part of the proglacial lake acted as a pinning point, and the glacier retreated only 0.14 km there between 1950 and 2000. Between 2000 and 2010, however, Sheridan Glacier began a catastrophic retreat, with much of the east part of the terminal lobe disintegrating into icebergs. Over this period, parts of the glacier retreated up to 1.3 km. Between 2010 and 2016, much of the remaining floating terminus disintegrated, retreating up to 1.6 km (Fig. 5). The far west edge of the terminus, however, has remained grounded since 1950. Maximum retreat of Sheridan Glacier between 1950 and 2016 is ~2.6 km.

The terminus of Sherman Glacier did not change as much as that of Sheridan Glacier over the same period (Fig. 5). Between 1950 and 1963, the year prior to the Alaska earthquake, the glacier retreated 0.2–0.5 km. Since then, landslide-induced changes in mass balance have caused Sherman Glacier to advance (McSaveney, 1975; Deline et al., 2014). Between 1969 and 1976, the southern part of the glacier terminus advanced up to 0.2 km, while the northern part changed little. Between 1976 and 1978, the north half of the terminus advanced about 0.07 km, while the south half remained stationary. Between 1978 and 1996, the entire terminus advanced, on average about 0.2 km; it advanced a further 0.04 km between 1996 and 2000, and up to ~0.05 km between 2000 and 2010. Signs of glacier advance were evident when we did our fieldwork in 2008 (Fig. 6). By 2016, the glacier advanced a further ~0.05 km, reaching its 1950 limit. While the Sherman Glacier terminus remains extended due to the insulating effects of the debris cover, the mass balance of the glacier is almost certainly negative. The snowline has been rapidly retreating over the past decade, and south-flowing tributaries have become detached from the trunk glacier due to thinning upvalley of the debris-covered terminus (Pelto, 2018).

The proglacial lakes, streams, and outwash plains draining Sheridan and Sherman glaciers have also changed markedly over

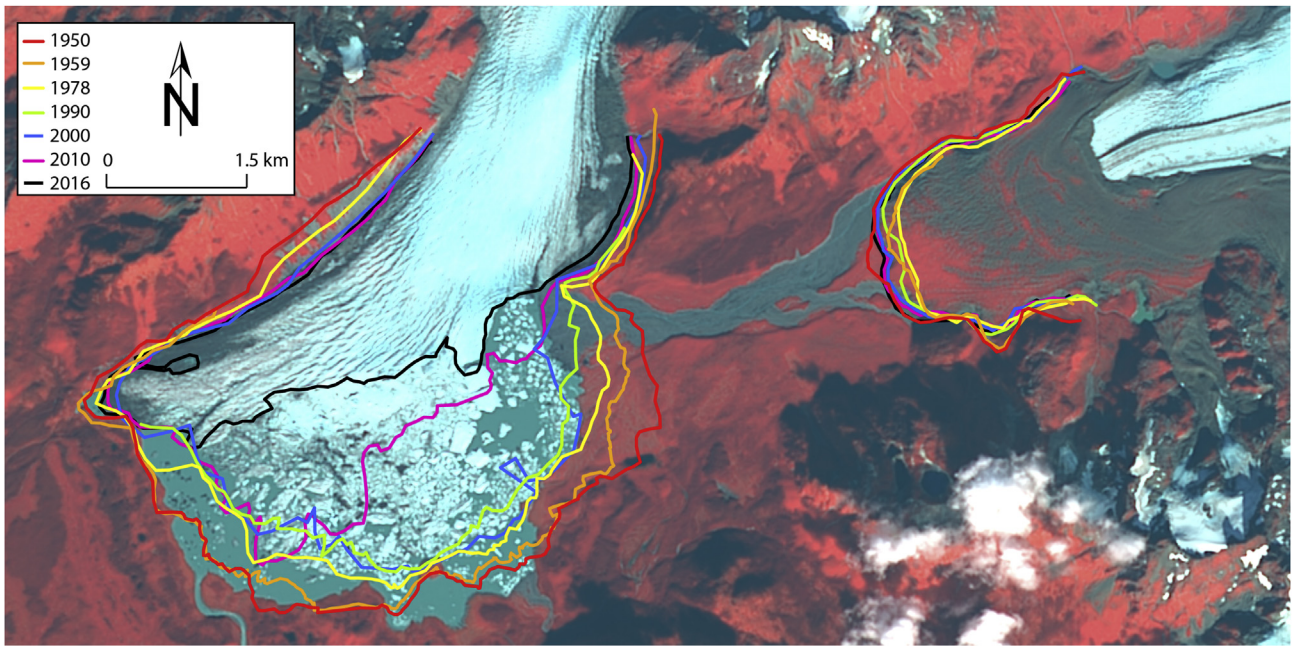

Fig. 5. Historic fluctuations of the termini of Sheridan and Sherman glaciers overlain on a pan-sharpened September 7, 2015 Landsat 8 image (NIR-G-B). Note that for clarity only select terminus positions are shown. (For interpretation of the references to colour in this figure legend, the reader is referred to the Web version of this article.)

Fig. 6. Photograph of the debris-covered terminus of Sherman Glacier in 2008, with author DHS (tending to blistered feet) for scale. Note the rumpled terrain and tilted saplings indicating advance of the glacier.

the historic record (Fig. 7). In 1950, meltwater flowed from Sheridan Glacier via a large braided river at the northwest edge of the terminus and out of a small proglacial lake via a small single-thread meandering stream near the middle of the terminus (Fig. 7A). A series of smaller proglacial lakes on the southeast and east sides of the terminus captured meltwater from Sherman Glacier and drained south via a third, meandering channel (Fig. 7B). By 1959, the small proglacial stream flowing from the middle of the glacier terminus had grown and begun to straighten in its proximal reaches, cutting off meanders and creating oxbow lakes (Fig. 7C). By 1974 (not shown), the proglacial lakes draining Sheridan Glacier had coalesced into a single large lake, and by 1978 the braided river draining the northwest corner of Sheridan Glacier had shrunk considerably (Fig. 7E). The channel of the meandering stream carrying Sherman Glacier meltwater was abandoned by 1974 (Fig. 7F; and fieldwork on Sherman Glacier by author MJM in 1974), leaving evidence of former point bars. Thereafter, meltwater from Sherman Glacier drained into Sheridan Glacier's large proglacial lake and then south via the braided channel to the west. Little substantive changes are evident between 1978 and 1997. However, by 2011 (not shown), the catastrophic retreat of Sheridan Glacier was underway, creating a much-enlarged proglacial lake (Fig. 5). Over the next five years, meltwater from Sheridan Glacier continued to discharge via the braided channel in the middle of the glacier forefield.

5. Discussion

Stratigraphic evidence and remote sensing analysis suggest that Sheridan Glacier has fluctuated markedly over the past two millennia, much more so than adjacent Sherman Glacier. Stumps buried in outwash suggest that Sheridan Glacier was advancing as early as cal. 220–380 CE (Sheridan 1). Subsequently, forest became established at the site of Sheridan 2, and conifers achieved ages of up to at least 210 years old based on a ring count on one stump. These trees died by cal. 540–620 CE (overlapping dates of Sheridan 2a and 2b). The Sheridan 2 site is likely close to the outermost limit of the First Millennium Advance in Sheridan Valley. In Sherman Valley, the tree stems at site C14-11 (overlapping dates of cal. 430–570 CE) occur within till, which marks the limit of Sheridan Glacier during the First Millennium Advance.

Tuthill et al. (1968) mention a glacier-pushed log dated to between cal. BC 40 and 780 CE (sample I-1986) at about the same distance from the present glacier terminus as our Sheridan 1 sample, although on the east side of the terminus. Barclay et al. (2013) argue that outwash from Sheridan Glacier killed many trees at their site 'D', located between our Sheridan 1 and Sheridan 2 sites (Fig. 1), from the 550s to 601 CE. They also describe interbedded outwash and till overlying these stumps, indicating that Sheridan Glacier advanced over the area at or soon after 609 CE. Zander et al. (2013) do not describe a glacier advance at this time, likely because no meltwater and thus no sediment entered Cabin Lake.

These interpretations likely correspond to the First Millennium

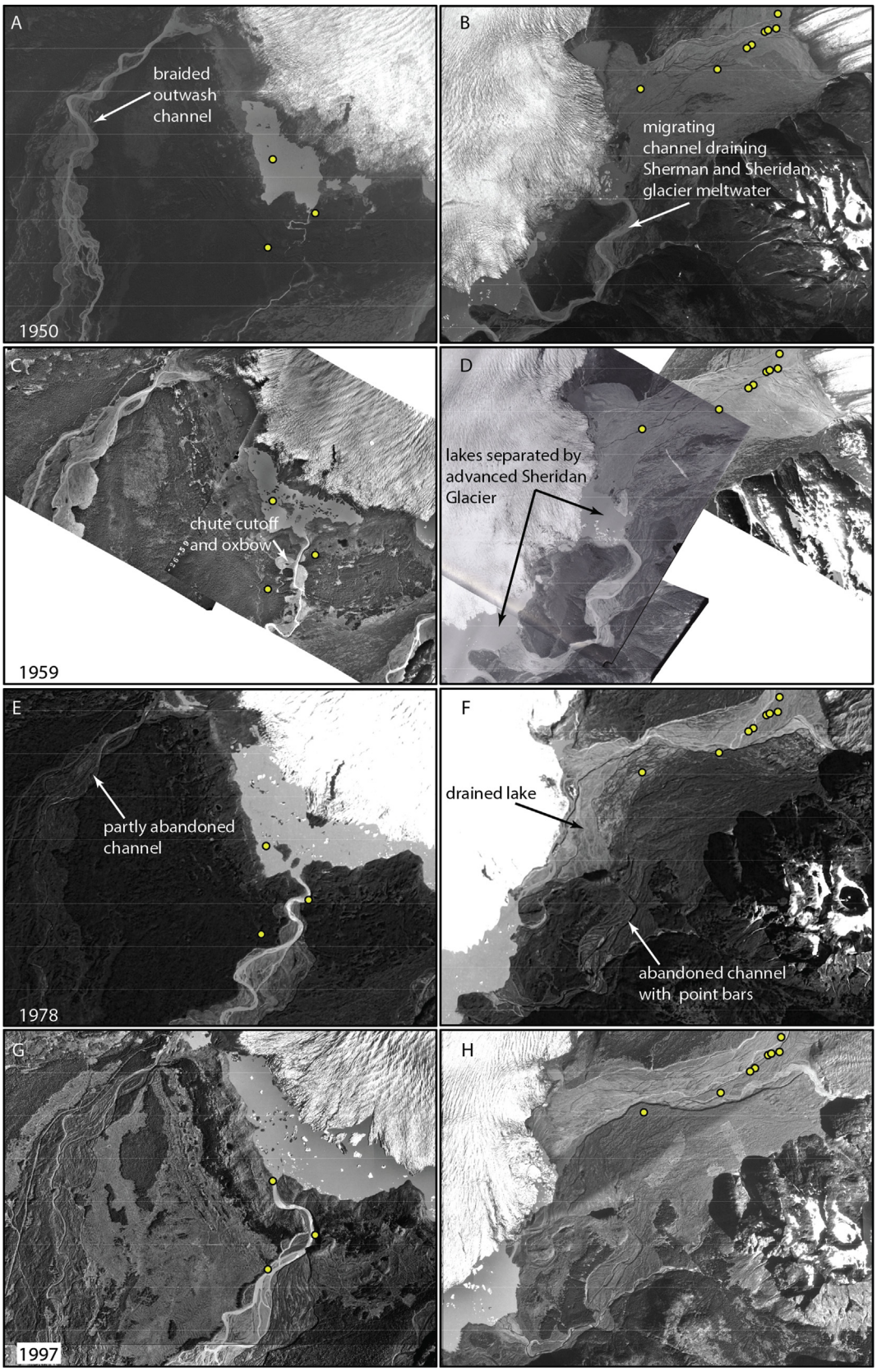

Fig. 7. Historic changes in the proglacial hydrology of Sheridan (left) and Sherman (right) glaciers. Yellow dots show locations of our radiocarbon-dated samples. (For interpretation of the references to colour in this figure legend, the reader is referred to the Web version of this article.)

Advance, which has been documented through the coastal region of northwest North America (Reyes et al., 2006). Reyes et al. (2006) infer two advances of glaciers during the First Millennium Advance, between cal. 210 and 570 CE. We cannot say for certain that the diachronous kill dates at Sheridan 1 and Sheridan 2 record separate advances, or rather different phases of a single advance.

We estimated the location of the glacier terminus during the First Millennium Advance in order to model lake formation at that time. In Fig. 8, Sheridan Glacier has expanded into Sherman valley (fifth or sixth century), depositing till from which samples C14-11B, 11D, and 11E came, and impounding a lake (~6.1×10^5 m^2) that drained over a spillway at about 140 m asl. It is possible that the lowest gravel at Sheridan 3 records one of these advances, although we have only a minimum limiting age for that unit. Barclay et al. (2013) argue, on the basis of forest growth on a bedrock knob just upstream of our Sheridan 3 (Fig. 1), that Sheridan Glacier retreated by 830–928 CE, following the First Millennium Advance.

The next advance of Sheridan Glacier was probably very early in the second millennium, although we did not find evidence for it ourselves. Zander et al. (2013) document floodplain aggradation between cal. 1110 and 1180 CE, and possibly again around cal. 1260 CE, but suggest that the advance responsible for the aggradation was less extensive than the First Millennium Advance. Barclay et al. (2013) cross-dated the outer ring of a single tree buried by outwash to 1156 CE. Peteet et al. (2016) attribute vegetation shifts in cores near Cabin Lake to retreat of Sheridan Glacier around 1200 CE.

The Sheridan 3 section provides evidence for four Holocene advances of the glacier – before cal. 1290 CE, shortly after cal. 1460 CE but before cal. 1480 CE, after cal. 1480 CE but before cal. 1680 CE, and after cal. 1680 CE but before the late 1700s CE. The cal. <1290 CE advance likely corresponds to that described by Barclay et al. (2013) as occurring between the 1240s and 1280s. The interval between the third and fourth advances was the longest, as the soil separating the two contained the largest trees in growth position, some up to 1 m in diameter that were likely more than 200 years old when they died (e.g., Sheridan 3C). The age range of Sheridan 3C, which marks the end of this event and renewed outwash deposition, is cal. 1480–1660 CE. The third advance inferred at Sheridan 3 corresponds to an advance of Sheridan Glacier beginning in the 1510s CE (Barclay et al., 2013), and to an advance of glaciers in the Kenai, Chugach, and Coast mountains between about 1540 and 1710 CE (Barclay et al., 2009). We suggest that Sheridan 3C, the tree dated by us, was buried in outwash in the eighteenth century based on the fact that sawn old-growth trees on the terrace above this dated stem show that no outwash was deposited on that surface since at least the late 1700s. Thus the final phase of outwash deposition, when Sheridan River aggraded to its highest level of the Holocene, probably occurred in the early or middle eighteenth century. At the LIA maximum, in the eighteenth century, Sheridan Glacier extended about 2.2 km up Sherman valley (from the current east edge of Sheridan Lake) and dammed another lake, albeit a small one due to reduced accommodation space between the advanced positions of Sheridan and Sherman glaciers (see Fig. 5 in Barclay et al., 2013).

Sherman Glacier did not fluctuate to the same extent as Sheridan Glacier during the past millennium (Fig. 9). We have no record of the activity of Sherman Glacier prior to the mid-fifteenth century, but Barclay et al. (2013) describe a hemlock stump that was buried in outwash near the present glacier terminus around cal. 1000 CE. Downvalley, several trees lived between 1360 and 1608 CE and were later buried by outwash. The stumps and logs on the Sherman River floodplain that we dated similarly record a period of stability during which local base level was at or below its present level prior to cal. 1630 CE (sample C14-7). Barclay et al. (2013) argue that Sherman Glacier was advancing to its Holocene maximum from the 1810s through 1830s CE.

Rapid aggradation of the floodplain, resulting in burial of conifers in Sherman River valley beneath up to 17 m of outwash, commenced after cal. 1635 CE and probably culminated in the nineteenth century. Aggradation was driven by a rise in base level controlled by the advance of Sheridan Glacier across Sherman River 2.5 km to the west. This advance would have impounded a lake in Sherman River valley. Base level rose 4 m before the end of the eighteenth century (C14-9) and probably 17 m less than 100 years later. Although the outwash sequence near Sherman Glacier is horizontally bedded, recording deposition on a braid plain, foreset beds were noted in exposures nearer Sheridan Glacier, indicating the presence of an ice-dammed lake in the lower part of the valley.

Retreat of Sheridan Glacier in the nineteenth and twentieth centuries enabled Sherman River to establish its channel at a lower

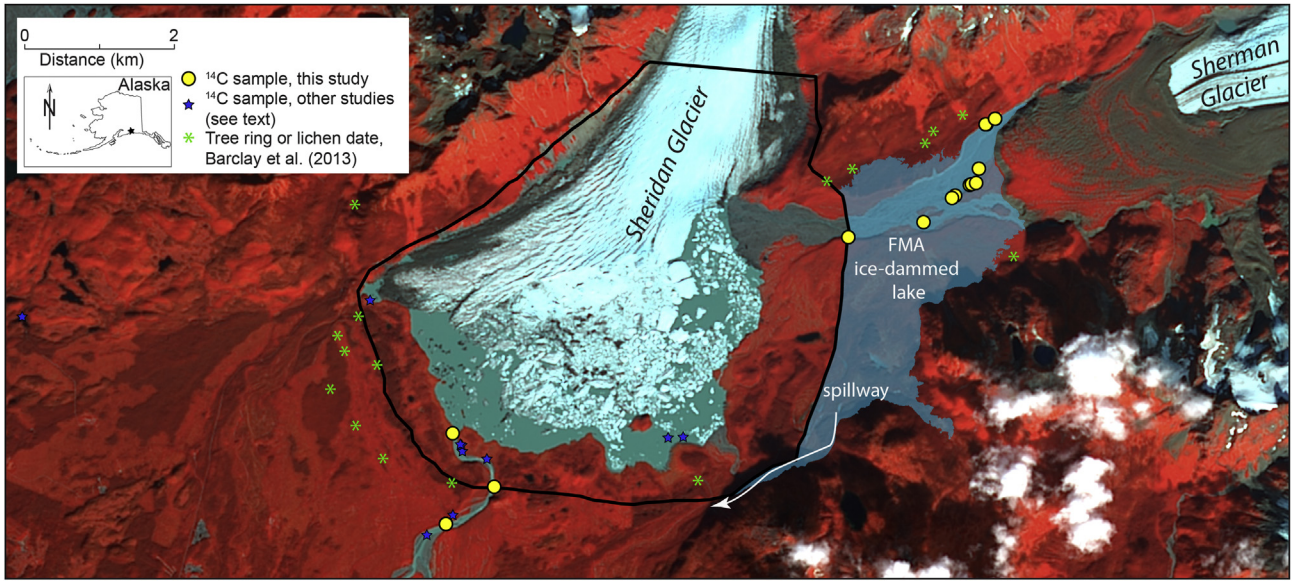

Fig. 8. Modelled glacier-dammed lake during the First Millennium Advance (thick black line). Base image is the same as for Fig. 1. Only fluctuations of Sheridan Glacier are shown for clarity.

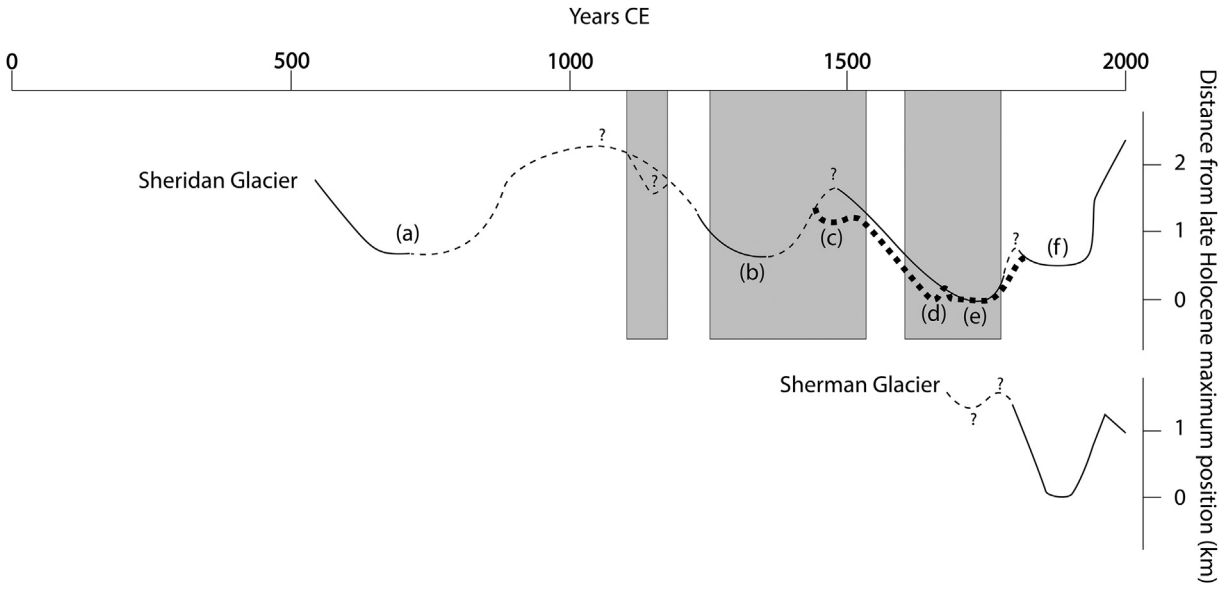

Fig. 9. Time-distance diagram for Sheridan and Sherman glaciers. Lightweight solid and dashed lines are reconstructions of Barclay et al. (2013), and heavyweight lines are our modifications. Grey boxes indicate intervals of glacier meltwater inflow to Cabin Lake from Zander et al. (2013). Labels (a) through (f) describe the six advances described in this study: (a) First Millennium Advance; (b) our cal. <1290 CE advance, which corresponds to that beginning in the 1240s-1280s CE described by (2013); (c) our advance after cal. 1460 CE but prior to cal. 1480 CE; (d) our advance after cal. 1480 CE but prior to cal. 1680 CE; (e) our advance from cal. 1680 CE to the late 1700s CE; and (f) the 1810–1860s CE advance of Barclay et al. (2013). Barclay et al.'s advance from 1510 to 1700 CE corresponds to our (d) and (e).

base level. The Sherman River valley fill, deposited only two centuries earlier, was rapidly dissected and removed. The sediments were carried into the expanding proglacial lake at the terminus of Sheridan Glacier. While this was happening, the terminus of Sherman Glacier was relatively stable. Photographs taken by David Barclay in 2002 (*pers. comm.*) indicate that the river had at that time not yet reached the level observed during our fieldwork in 2008, indicating a rapidly evolving landscape.

6. Conclusion

We infer the recent activity of Sheridan and Sherman glaciers, two adjacent glaciers in the Chugach Mountains of southeast Alaska. Based on our own work and that of previous researchers, we infer five or possibly six advances of Sheridan Glacier in the past 1500 years. These include (a) a First Millennium Advance, which was also described by previous workers; (b) an advance prior to 1290 CE, likely the same as that from the 1240s-1280s described previously; (c) an advance after 1460 but prior to 1480 CE; (d) an advance after 1480 but prior to 1680 CE; (e) an advance from 1680 to the late 1700s CE; and (f) an advance between 1810 and the 1860s CE that was described previously. Our advances (d) and (e) are possibly different phases of a single advance.

Sherman Glacier thickened and advanced at the same time as Sheridan Glacier during the last of these advances during the classical Little Ice Age. The pre-LIA activity of Sherman Glacier remains unknown. The response of the two glaciers to twentieth and early twenty-first century warming, however, has been very different. Sheridan Glacier has retreated up to 3 km since the early 1900s, most of it during the past 70 years. In contrast, Sherman Glacier has retreated less than 1 km from its Little Ice Age limit. It retreated 0.5–0.7 km between 1950 and 1963, but since then has re-advanced to near its 1950 limit. In the past decade, Sherman Glacier has experienced a negative mass balance due mainly to thinning upvalley; however, its terminus has not yet responded.

At least two factors are responsible for the recent differences in the activity of the two glaciers. First, a rock avalanche in 1964 covered much of the lower part of Sherman Glacier with a blanket of blocky debris, which reduced the loss of ice in the ablation area and had generated a slightly positive mass balance that has allowed the glacier to advance while neighbouring Sheridan Glacier continued to retreat. Second, a lake began to develop at the terminus of Sheridan Glacier around 1950, leading to large ice losses by calving. Calving-related losses of ice at the terminus of Sheridan Glacier have increased over the past ten years. The landscape around the two glaciers has also changed dramatically during and since the Little Ice Age. Sheridan Glacier advanced sufficiently during the Little Ice Age to block the mouth of Sherman valley and impound a lake that extended back to the Sherman Glacier terminus. The lake became infilled with outwash, raising base level in Sherman valley about 17 m by the end of the nineteenth century. Over the past century, as the mouth of the valley became ice-free, much of this outwash was removed and base level lowered, a process that may be continuing.

Acknowledgments

We thank Mark Irving and Alaska River Rafters for logistics support. Financial support for the fieldwork and analysis was provided by: NSERC (Discovery Grant 24595) and the Canada Research Chairs program to JJC; an NSERC-PGS-D3 scholarship, SFU Graduate International Scholarship, Northern Scientific Training Program grant, Arctic Institute of North America Grant-in-Aid, and Geological Society of America 'Bruce L. Reed' Research Award to DHS; and support from GNS Science, New Zealand, to MJM. DEMs provided by the Polar Geospatial Center under NSF OPP awards 1043681, 1559691 and 1542736 were created from DigitalGlobe, Inc. imagery. Two anonymous reviewers helped guide the paper to its current state.

Appendix A. Supplementary data

Supplementary data related to this article can be found at https://doi.org/10.1016/j.quascirev.2018.07.016.

Appendix 1. List of aerial photographs and satellite images used (satellite image italicized).

Year	Photo ID	Tiepoints	RMSE (m)	Georeferenced resolution (m)
1950	USGS_3FYL11021_074	14	6.83	3.93
	USGS_3FYL11021_075	13	4.93	3.55
	USGS_3FYL11021_043	13	5.73	4.08
	USGS_3FYL11021_044	15	11.61	3.48
	USGS_3FYL11021_035	14	11.32	3.81
	USFS_Sheridan_1950_part1	12	2.44	11.59
	USFS_Sheridan_1950_part2	11	1.75	10.86
1959	USFS_6_12_59_EEV_16_180_400	11	2.20	1.46
	USFS_6_12_59_EEV_17_13_400	11	2.02	1.31
	USFS_6_12_59_EEV_17_150	14	8.31	2.02
	USFS_6_12_59_EEV_17_149	14	8.31	2.15
	USFS_5_26_59_EEV_7_194	12	3.04	2.03
	USFS_5_26_59_EEV_7_195	13	5.33	2.03
	USFS_5_26_59_EEV_7_196	13	3.82	2.00
	USFS_5_26_59_EEV_7_197	13	5.77	2.14
1963	OhioState_Sherman_8_27_63	15	7.09	2.30
1969	OhioState_Sherman_8_25_69	20	20.60	2.04
1974	USFS_Sheridan_7_17_74_0043_774_133	11	6.83	2.02
	USFS_Sheridan_7_17_74_0043_774_134	11	1.07	1.93
	USFS_Sheridan_7_17_74_0043_139	11	1.05	1.96
	USFS_Sheridan_7_17_74_0044_974_065	12	2.17	1.89
	USFS_Sheridan_8_16_74_0042_974_36	13	5.91	1.91
	USFS_Sheridan_8_16_74_0042_974_38	12	6.09	2.04
1976	USGS_5SYL05031_057	19	15.21	14.11
	USGS_5SYL05022_107	13	3.91	6.23
	USGS_8GGY09042_035	17	12.44	2.63
	USGS_8GGY09042_015	13	1.68	2.51
	USGS_8GGY09042_081	11	4.74	2.42
	USGS_8GGY09042_082	12	5.07	2.36
1978	USGS_5RBL08031_088	12	3.57	5.70
	USGS_5RBL08042_048	17	9.21	9.83
1982	USGS_8EGY04021_045	13	2.19	5.71
	USFS_Sheridan_Aug82_1515	12	2.41	5.96
	USFS_Sheridan_Aug82_1516	11	1.84	5.67
1983	USGS_8FWT02021_040	17	5.58	5.90
	USGS_8FWT02021_041	20	5.70	5.97
	USFS_Sheridan_July83_4407	16	4.93	5.87
	USFS_Sheridan_July83_4408	14	7.77	5.85
1985	USGS_8HTQ08041_166	16	5.30	6.99
	USGS_8HWT06052_092	13	8.05	14.21
	USGS_8HWT06052_093	16	6.52	11.65
1986	USFS _7_10_86_301	13	3.65	1.99
	USFS _7_10_86_302	14	3.31	1.88
	USFS _7_10_86_303	15	5.58	1.96
1990	NSIDC_USGS_90V1_164	12	4.10	1.78
	NSIDC_USGS_90V1_163	11	2.57	1.81
	NSIDC_USGS_90V1_162	12	6.42	1.85
	NSIDC_USGS_90V1_161	13	5.30	1.70
	NSIDC_USGS_90V1_160	13	8.54	1.73
	NSIDC_USGS_90V1_159	11	3.64	1.60
1996	USGS_8QT0252_009	15	5.98	5.79
	USGS_8QT0252_102	12	3.51	5.64
	USGS_8QT0252_103	18	7.97	5.83
	USFS _7_16_96_0007	15	3.34	5.76
	USFS _7_16_96_0101	13	6.05	5.84
1997	DOQQ.USFS.Chugach. 1996_2004.CRDB3NW	n/a	n/a	2.00
	DOQQ.USFS.Chugach. 1996_2004.CRDB4NE	n/a	n/a	2.00
	DOQQ.USFS.Chugach. 1996_2004.CRDB4NW	n/a	n/a	2.00
	DOQQ.USFS.Chugach. 1996_2004.CRDB3SE	n/a	n/a	2.00
	DOQQ.USFS.Chugach. 1996_2004.CRDB3SW	n/a	n/a	2.00
	DOQQ.USFS.Chugach. 1996_2004.CRDB4SE	n/a	n/a	2.00
	DOQQ.USFS.Chugach. 1996_2004.CRDB4SW	n/a	n/a	2.00
2000	*Landsat_ETM-N-06-60_2000*	n/a	n/a	14.25
	LE70650182000274AGS00	n/a	n/a	15.00
2010	*LE70650182010253EDC00*	n/a	n/a	15.00
2011	*SPOT5_Aug28_2011*	14	4.68	2.57
2016	*LC80660182016173LGN00*	n/a	n/a	15.00

References

Abercrombie, W.R., 1900. Supplementary expedition into the Copper River valley, Alaska. In: Compilation of Narratives of Explorations in Alaska. Government Printing Office, Washington, DC. Number of 383–408 pp.

Barclay, D.J., Wiles, G.C., Calkin, P.E., 2009. Holocene glacier fluctuations in Alaska. Quat. Sci. Rev. 28, 2034–2048.

Barclay, D.J., Yager, E.M., Graves, J., Kloczko, M., Calkin, P.E., 2013. Late Holocene glacial history of the Copper River Delta, coastal south-central Alaska, and controls on valley glacier fluctuations. Quat. Sci. Rev. 81, 74–89.

Bolch, T., Kulkarni, A., Kääb, A., Huggel, C., Paul, F., Cogley, J.G., Frey, H., Kargel, J.S., Fujita, K., Scheel, M., Bajracharya, S., Stoffel, M., 2012. The state and fate of Himalayan glaciers. Science 336, 310–314.

Bolch, T., Menounos, B., Wheate, R., 2010. Landsat-based inventory of glaciers in western Canada, 1985-2005. Rem. Sens. Environ. 114, 127–137.

Bronk Ramsey, C., 2009. Bayesian analysis of radiocarbon dates. Radiocarbon 51, 337–360.

Clarke, G.K.C., Anslow, F.S., Jarosch, A.H., Radić, V., Menounos, B., Bolch, T., Berthier, E., 2012. Ice volume and subglacial topography for western Canadian glaciers from mass balance fields, thinning rates, and a bed stress model. J. Clim. 121221142118006.

Deline, P., Hewitt, K., Reznichenko, N., Shugar, D.H., 2014. Rock avalanches onto glaciers. In: Davies, T. (Ed.), Landslide Hazards, Risks, and Disasters. Elsevier, Amsterdam. Number of 263–320 pp.

Dyurgerov, M.B., Meier, M.F., 2000. Twentieth century climate change: evidence from small glaciers. Proc. Natl. Acad. Sci. Unit. States Am. 97, 1406–1411.

Gardelle, J., Berthier, E., Arnaud, Y., 2012. Slight mass gain of Karakoram glaciers in the early twenty-first century. Nat. Geosci. 5, 322–325.

Grant, U.S., Higgins, D.F., 1909. Copper mining and prospecting on Prince William Sound. In: U.S. Geological Survey Bulletin 379-C, pp. 87–152.

Grove, J.M., 2008. The Little Ice Age. Routledge, New York.

Hobbs, W.H., 1911. Characteristics of Existing Glaciers. The Macmillan Company, New York.

Hoffman, K.M., Smith, D.J., 2013. Late Holocene glacial activity at Bromley Glacier, Cambria Icefield, northern British Columbia Coast mountains, Canada. Can. J. Earth Sci. 50, 599–606.

Key, C.H., Fagre, D.B., Menicke, R.K., 2002. glacier retreat in Glacier National Park, Montana. In: Williams, R.S.J., Ferrigno, J.G. (Eds.), Satellite Image Atlas of Glaciers of the World. Glaciers of North America U.S. Geological Survey Professional Paper 1386-J-1, Number of J365–J381 pp.

Lutz, H.J., 1930. Observations on the invasion of newly formed glacial moraines by trees. Ecology 11, 562–567.

Marangunic, C., Bull, C., 1968. The landslide on the Sherman glacier. In: The Great Alaska Earthquake of 1964-Hydrology, Pt. A. National Academy of Sciences, Washington, DC. Number of 383–394 pp.

Mayo, L., 1989. Advance of Hubbard Glacier and 1986 outburst of Russell Fiord, Alaska. Ann. Glaciol. 13, 189–194.

McSaveney, M.J., 1975. The Sherman Glacier Rock Avalanche of 1964: its Emplacement and Subsequent Effects on the Glacier beneath it. Ph.D. Ohio State University, Columbus, OH, p. 403.

McSaveney, M.J., 1978. Sherman Glacier rock avalanche, Alaska, U.S.A. In: Voight, B. (Ed.), Rockslides and Avalanches, 1 Natural Phenomena. Elsevier, Amsterdam. Number of 197–258 pp.

Moore, R.D., Fleming, S.W., Menounos, B., Wheate, R., Fountain, A., Stahl, K., Holm, K., Jakob, M., 2009. Glacier change in western North America: influences on hydrology, geomorphic hazards and water quality. Hydrol. Proced. 23, 42–61.

Motyka, R.J., Echelmeyer, K., 2003. Taku Glacier (Alaska, U.S.A.) on the move again: active deformation of proglacial sediments. J. Glaciol. 49, 50–58.

Owen, L.A., Dortch, J.M., 2014. Nature and timing of Quaternary glaciation in the Himalayan–Tibetan orogen. Quat. Sci. Rev. 88, 14–54.

Pelto, M., 2018. Sherman Glacier, Alaska diminishing protective blanket = mass loss. https://blogs.agu.org/fromaglaciersperspective/2018/05/29/sherman-glacier-alaska-diminishing-protective-blanketmass-loss/. (Accessed 25 June 2018).

Peteet, D.M., Nichols, J.E., Moy, C.M., McGeachy, A., Perez, M., 2016. Recent and Holocene climate change controls on vegetation and carbon accumulation in Alaskan coastal muskegs. Quat. Sci. Rev. 131, 168–178.

Reyes, A.V., Wiles, G.C., Smith, D.J., Barclay, D.J., Allen, S., Jackson, S., Larocque, S., Laxton, S., Lewis, D., Calkin, P.E., Clague, J.J., 2006. Expansion of alpine glaciers in Pacific North America in the first millennium AD. Geology 34, 57–60.

Roe, G.H., Baker, M.B., Herla, F., 2017. Centennial glacier retreat as categorical evidence of regional climate change. Nat. Geosci. 10, 95–99.

Seton-Karr, H.W., Bremner, J., 1887. The Shores and Alps of Alaska. Sampson Low. Marston, Searle, & Rivington, London.

Shugar, D.H., Clague, J.J., 2011. The sedimentology and geomorphology of rock avalanche deposits on glaciers. Sedimentology 58, 1762–1783.

Shugar, D.H., Clague, J.J., Best, J.L., Schoof, C., Willis, M.J., Copland, L., Roe, G.H., 2017. River piracy and drainage basin reorganization led by climate-driven glacier retreat. Nat. Geosci. 10, 370–375.

Shugar, D.H., Rabus, B.T., Clague, J.J., 2010. Elevation changes (1949-1995) of Black Rapids Glacier, Alaska, derived from a multi-baseline InSAR DEM and historical maps. J. Glaciol. 56, 625–634.

Solomina, O.N., Bradley, R.S., Hodgson, D.A., Ivy-Ochs, S., Jomelli, V., Mackintosh, A.N., Nesje, A., Owen, L.A., Wanner, H., Wiles, G.C., Young, N.E., 2015. Holocene glacier fluctuations. Quat. Sci. Rev. 111, 9–34.

Solomina, O.N., Bradley, R.S., Jomelli, V., Geirsdottir, A., Kaufman, D.S., Koch, J., McKay, N.P., Masiokas, M., Miller, G., Nesje, A., Nicolussi, K., Owen, L.A., Putnam, A.E., Wanner, H., Wiles, G., Yang, B., 2016. Glacier fluctuations during the past 2000 years. Quat. Sci. Rev. 149, 61–90.

St-Hilaire, V.M., Smith, D.J., 2017. Holocene glacier history of Frank Mackie Glacier, northern British Columbia Coast Mountains. Can. J. Earth Sci. 54, 76–87.

Tarr, R.S., Martin, L., 1914. Alaskan Glacier Studies of the National Geographic Society in the Yakutat Bay, Prince William Sound and Lower Copper River Regions. National Geographic Society, Washington, DC.

Tuthill, S.J., Field, W.O., Clayton, L., 1968. Postearthquake studies at Sherman and Sheridan glaciers. In: The Great Alaska Earthquake of 1964-Hydrology, Pt. A. National Academy of Sciences, Washington, DC. Number of 318–328 pp.

Wentworth, C.K., Ray, L.L., 1936. Studies of certain Alaskan glaciers in 1931. Geol. Soc. Am. Bull. 47, 879–934.

Wiles, G.C., Barclay, D.J., Calkin, P.E., 1999. Tree-ring-dated 'Little Ice Age' histories of maritime glaciers from western Prince William Sound, Alaska. Holocene 9, 163–173.

Wiles, G.C., Barclay, D.J., Calkin, P.E., Lowell, T.V., 2008. Century to millennial-scale temperature variations for the last two thousand years indicated from glacial geologic records of Southern Alaska. Global Planet. Change 60, 115–125.

Zander, P.D., Kaufman, D.S., Kuehn, S.C., Wallace, K.L., Anderson, R.S., 2013. Early and late Holocene glacial fluctuations and tephrostratigraphy, Cabin Lake, Alaska. J. Quat. Sci. 28, 761–771.